Free energy of defect formation: Thermodynamics of anion Frenkel pairs in indium oxide

Aron Walsh,[1,*] Alexey A. Sokol,[2] and C. Richard A. Catlow[2]

[1]*Centre for Sustainable Chemical Technologies and Department of Chemistry, University of Bath, Claverton Down, Bath BA2 7AY, United Kingdom*

[2]*University College London, Kathleen Lonsdale Materials Chemistry, Department of Chemistry, 20 Gordon Street, London WC1H 0AJ, United Kingdom*

(Received 5 November 2010; revised manuscript received 29 March 2011; published 21 June 2011)

The temperature-dependent free energies, entropies, and enthalpies for the formation of anion Frenkel pairs in In_2O_3 are reported, as calculated within the Mott-Littleton embedded-cluster approach, by exploiting the relationship between isobaric and isochoric thermodynamic processes. Our model for In_2O_3 proves particularly successful in the reproduction and prediction of the thermoelastic properties, including heat capacity, compressibility, and thermal expansion in the high-temperature regime. We employ this model to predict the thermal behavior of oxygen vacancy and oxygen interstitial defects. Aggregation of the point defects is energetically favorable and dampens the temperature dependence of defect formation, with a decreased free volume of defect formation. The results highlight the contribution of point defects to the high-temperature thermal expansion of indium sesquioxide, as well as the appreciable temperature dependence of the thermodynamic potentials, including enthalpy and free energy, associated with defect formation in general. A transferable procedure for calculating such thermodynamic parameters is presented.

DOI: 10.1103/PhysRevB.83.224105 PACS number(s): 61.72.jn, 71.20.−b, 77.84.Bw, 65.40.De

I. INTRODUCTION

Indium sesquioxide has been a leading transparent conducting metal oxide (TCO) for the past forty years.[1] The combination of optical transparency with electronic conductivity makes TCOs desirable for electrochromic, photovoltaic, and a range of other optoelectronic applications.[2–4] Despite the great importance of In_2O_3, our understanding of its defect properties is far from complete, especially considering their crucial role in determining its physicochemical properties. Based on the measured dependence of electrical conductivity and oxygen partial pressure at high temperatures, De Wit suggested that oxygen vacancies were the dominant ionic defects,[5] while Ohya *et al*. recently proposed that oxygen loss leads to a defect complex comprising interstitial In and O pairs;[6] the reported powers for the conductivity dependence span from $p_{O_2}^{-1/5}$ to $p_{O_2}^{-1/10}$, indicating the complex nature of the defect chemistry occurring in this system.[5–8] Previous theoretical studies of In_2O_3 have concentrated on defect reactions involving isolated oxygen vacancies and indium interstitials for generating intrinsic electron charge carriers,[9–13] and more recently on ion transport through the lattice.[14]

We have recently developed an analytical interatomic potential for In_2O_3 that provides a good description of the structural, dielectric, and elastic properties of the thermodynamically stable phase of In_2O_3 (bixbyite), as well as a number of high-pressure phases[15] and nanoclusters;[16] the Buckingham pairwise potential is supplemented with shell model polarization of oxygen, and full details of the parametrization can be found in Ref. 15. The pertinent equilibrium properties are summarized in Table I. From an investigation of a range of stoichiometric defect reactions, we previously identified anion Frenkel pairs as the lowest energy source of stoichiometry-preserving intrinsic ionic disorder:

$$O_O \rightleftharpoons V_O^{\bullet\bullet} + O_i^{//}, \tag{1}$$

in which the defects are represented using the standard notation of Kröger and Vink, where the perfect lattice is considered as a neutral reference, and positive and negative charges on defect sites are represented by dots and dashes, respectively. The reaction energy is calculated from

$$E_{\text{Frenkel}} = \tfrac{1}{2}(E[V_O^{\bullet\bullet}] + E[O_i^{//}]) = 3.19\ \text{eV} \tag{2}$$

per defect, where $E[V_O^{\bullet\bullet}]$ and $E[O_i^{//}]$ represent the energetic cost of introducing the corresponding isolated charged point defect into the bulk lattice at infinite dilution. For this balanced defect reaction, the total number of ions remains fixed and no external chemical potential is required.

Frenkel disorder is favored because the thermodynamically stable phase of In_2O_3 contains intrinsic structural anion vacancies that facilitate interstitial formation on the 16*c* Wyckoff position; the bixbyite crystal structure can be viewed as a $2 \times 2 \times 2$ supercell of the cubic fluorite (CaF_2) structure with ordered anion vacancies. At high temperatures, disorder in the anion sublattice of the bixbyite structure has been reported, consistent with significant concentrations of anion Frenkel pairs.[17] Moreover, for samples with high electron carrier concentrations, such as heavily Sn-doped In_2O_3 (ITO), charged oxygen interstitials are known to be present as compensating defect centers.[18]

While no studies of stoichiometric defect reactions have been reported based on electronic structure techniques, an anion Frenkel-pair energy of 2.89 eV can be calculated from the defect formation energies reported by Ágoston *et al*.[10] at the level of GGA + U in a periodic supercell, which is in reasonable agreement with our reported value of 3.19 eV.

Although it has become standard practice to focus on the calculation of defect formation energies under constant volume (isochoric) conditions at $T = 0$ K,[9–13,19–29] the thermodynamic processes determining equilibrium defect concentrations are related to the Gibbs free energy of the defect reaction, defined under constant pressure (isobaric) conditions at finite

TABLE I. Calculated and empirical properties of the bixbyite phase of In_2O_3 obtained using an interatomic potential model[15] and density functional theory (DFT). The PBEsol-DFT values of ϵ_S and ϵ_∞ are calculated without the inclusion of LO-TO splitting or additional corrections to the Kohn-Sham band gap.

Property	Potential Model (This study)	Experiment	LDA-DFT[59]	PBEsol-DFT (This study)
Lattice constant (Å)	10.121	10.117[60]	10.094	10.172
Bulk modulus (GPa)	193.77	194.24[61]	174	157.10
Compressibility ($\times 10^{-3}$ GPa^{-1})	5.16	5.15[61]	5.75	6.37
Heat capacity (C_p°, J mol^{-1}K^{-1})	102.17	99.08[62]		
Static dielectric constant (ϵ_S)	9.05	8.9 − 9.5[3]		6.02
Optical dielectric constant (ϵ_∞)	3.90	4.0[3]	3.82[a]	4.82

[a]The reported value includes an *a posteriori* correction to the LDA band gap based on a separate HSE03+G_0W_0 calculation.

temperatures: $G_d = H_d - TS_d$. The importance of temperature and volume for the free energies of defect formation has long been recognized.[30] When it was incorporated into defect calculations, more than thirty years ago, the resulting model was able to reproduce successfully the known high-temperature defect behavior of silver halides,[31–33] as well as other ionic systems.[34–36] In_2O_3 represents a particularly interesting case as it exhibits significant variation in its high-temperature physicochemical properties, including lattice constant and conductivity.[8,17,37,38]

Theoretical approaches to the calculation of defect formation enthalpies and free energies have generally been performed within the quasiharmonic approximation by combining a temperature-independent interatomic potential with the temperature-dependent lattice constants and dielectric properties taken from experiment.[34–36,39–41] Anharmonic effects become relevant close to the melting point as demonstrated in a recent computational study by Grabowski *et al.*,[42] which addressed the issue of vacancy formation on the free-energy surface of aluminium at high temperatures, and included anharmonicity through explicit thermodynamic integration.

A key quantity is the isochoric pressure change on defect formation [$p_d = -(\frac{\partial A_d}{\partial V})_T$], which can be calculated from the derivative of the Helmholtz free energy ($A_d = U_d - TS_d$) of the defect reaction with respect to the lattice volume. Conceptually, this pressure is an isotropic measure of the stress exerted by the defect that should result in a lattice (elastic) strain, which in turn is released under constant pressure. Improved computational resources allow us to remove a number of the previous approximations,[31–36] and compute the temperature-dependent elastic and dielectric properties of the bulk material directly by calculating explicitly the vibrational contributions, and minimizing free energy with respect to all structural degrees of freedom. The salient details of this approach are presented in this work, and it is applied to a pertinent point-defect pair and its bound complex in In_2O_3. The results highlight the role of defects in the lattice-constant expansion of In_2O_3 at high temperatures, and provide further insight into the complex defect chemistry of this material.

II. THEORETICAL AND COMPUTATIONAL APPROACHES

The bulk and defect properties of In_2O_3 were calculated using a set of optimized interatomic potentials[15] within the code GULP.[43] Thermoelastic effects of the bixbyite lattice (40-atom body-centered cubic unit cell) were investigated by minimizing the free energy as a function of temperature within the quasiharmonic approximation: at each temperature, free-energy minimization is performed over all structural degrees of freedom, using the internal lattice energy (U) and the vibrational contributions obtained from the phonon density of states.[44,45] A $8 \times 8 \times 8$ Monkhorst-Pack k-point mesh,[46] sampling over the first Brillouin zone, was found to offer convergence in the free energies of up to 1×10^{-5} eV and in the cell volumes of 1×10^{-4} Å^3. Temperature-dependent properties were investigated from 0 to 1500 K in steps of 20 K; this is well below the experimental melting point of In_2O_3, which is in excess of 2000 K, so that the quasiharmonic approximation remains valid.

All calculations of the defect properties were performed within the embedded-cluster, Mott-Littleton method[47] to provide an accurate description of the infinitely dilute limit: the simulation is divided into an inner region in which interactions are explicitly treated (region I), and an outer region that responds to the defect perturbation via a linear response approach (region II). The radius of region I was chosen as 15 Å (>1000 atoms) with a 30 Å radius for the region IIa (>9000 atoms). The region IIb continuum commences outside these spheres and extends to infinity. A complete shell (electronic polarization) and ionic relaxation of region I was performed. A similar multiregion approach can also be used with electronic-structure techniques, e.g., as implemented in the CHEMSHELL package,[48,49] as was recently applied to assess the doping limits of ZnO.[50] To facilitate the automated calculation of the key thermodynamic parameters associated with defect formation, including entropies, enthalpies, and free energies, we have implemented our approach within the auxiliary code FREE.

To validate our interatomic pair-potential model, supplementary calculations of the structural and vibrational properties of bulk In_2O_3 were performed using density functional theory[51,52] as implemented in the code VASP,[53–55] with the exchange-correlation functional of Perdew, Burke, and Ernzerhof revised for solids (PBEsol).[56] A plane-wave cut-off of 500 eV and a k-point grid of $3 \times 3 \times 3$ were found to be well converged. The equilibrium lattice constant and bulk modulus were obtained from the energy-volume data from a series of constant-volume calculations, and a fit to the Murnaghan equation of state;[57] the final forces were minimized to below

0.001 eV/Å. The phonon frequencies at the Γ point were determined from the interatomic-force constant matrix obtained through density functional perturbation theory (DFPT), which also enabled the calculation of the optical (ϵ_∞) and static (ϵ_S) dielectric constants using a $9 \times 9 \times 9$ k-point mesh across the first Brillouin zone; due to the band-gap underestimation at the PBEsol level and the neglect of the vibrational splitting of transverse and longitudinal optical modes (so-called LO-TO splitting), the errors in both dielectric constants are relatively large, as shown in Table I. Both sources of error could be overcome in the near future when suitable, currently available, techniques are implemented and become tractable (cf. Ref. 58).

III. RESULTS

A. Bulk thermoelastic properties

Before addressing the temperature dependence of the defect reaction formation energies and enthalpies, we must first understand and quantify the thermoelastic properties of the bulk host metal oxide itself.

1. Phonon dispersion

The optical-phonon dispersion, calculated at T = 0 K using the interatomic pair potential, ranges from 107 to 545 cm^{-1} at the Γ point, as shown in Fig. 1, which includes a description of the LO-TO splitting. The LO-TO splitting is largest in the high-frequency range, which raises a vibrational mode from a triply degenerate state at 512 to 545 cm^{-1}. In comparison, the Γ-point frequencies calculated from the first-principles DFPT approach range from 75 to 555 cm^{-1}, in good overall agreement, but indicative of a slightly harder energy surface for the interatomic potential model. Recently, DFPT calculations of the lattice dynamics of the related metal oxide Cu_2O, using a similar exchange-correlation functional, have shown excellent agreement with neutron-scattering experiments.[63]

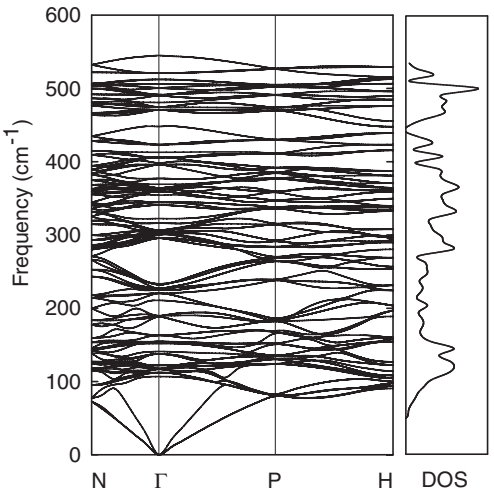

FIG. 1. Calculated phonon dispersion and density of states (DOS) of the bixbyite phase of In_2O_3 using a classical interatomic potential. The primitive body-centered cubic unit cell contains 40 atoms with 120 ($3N$) vibrational modes.

2. Linear thermal expansion

The linear thermal-expansion coefficient is defined as:

$$\alpha_l = \frac{1}{a_0}\left(\frac{\partial a}{\partial T}\right)_p, \tag{3}$$

where a_0 is the lattice constant at the initial temperature. The thermal expansion of In_2O_3 was first measured by Weiher and Ley[37] through dilation experiments, who observed that single-crystal and powdered samples exhibit a similar temperature dependence from 0 to 700 °C when heated in air. The lattice constant fits well to a polynomial of the form $a = a_0(1 + \alpha T + \alpha' T^2)$, with $\alpha = 6.15 \times 10^{-6}$ °C^{-1} and $\alpha' = 3.15 \times 10^{-9}$ °C^{-2}. A subsequent high-temperature x-ray diffraction (XRD) study by Kundra and Ali[38] on powder samples heated in vacuum up to 968 °C reported a fit of $\alpha = 7.2 \times 10^{-6}$ and $\alpha' = 1.15 \times 10^{-9}$. Later work by Solov'eva[17] on polycrystalline samples heated both in air and in vacuum reported a linear expansion coefficient of $\alpha = 7.5 \times 10^{-6}$ for stoichiometric In_2O_3, which decreased to 5.92×10^{-6} in the 550–1100 °C range. Data from the three experiments are reproduced in Fig. 2. Up to 550 °C, the measurements are consistent, but at higher temperatures the quadratic ($\alpha' T^2$) terms contribute to the steeper rise in the lattice expansion measured by Weiher and Ley and Kundra and Ali in comparison to the work of Solov'eva.

From the structure-temperature data calculated using our interatomic potential model, α_l can be extracted from a plot of the relative change in lattice constant ($\Delta a/a_0$) against temperature (T), which is also shown in Fig. 2. The predicted expansion of the perfect bulk lattice by the interatomic potential is less pronounced than that of experiment ($\alpha = 4.44 \times 10^{-6}$ and $\alpha' = 7.99 \times 10^{-10}$) in the low-temperature range. However, in the 550–1100 °C range measured by Solov'eva, the calculated expansion of 5.85×10^{-6} °C^{-1} compares very well to the measured value of 5.92×10^{-6} °C^{-1}. We find that in this

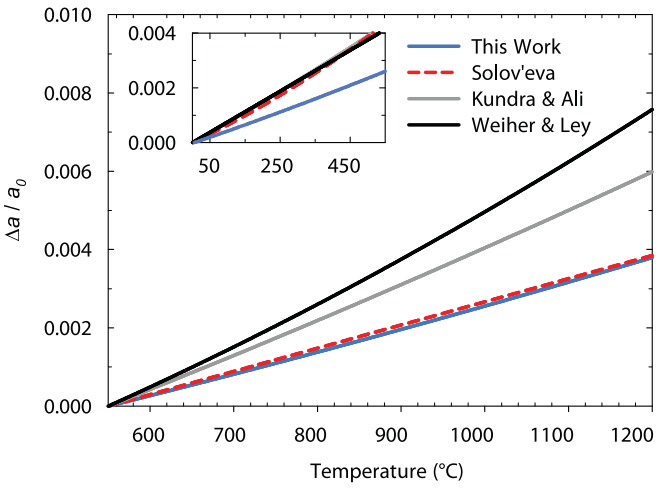

FIG. 2. (Color online) Calculated linear thermal expansion of bulk In_2O_3 in the bixbyite structure (solid line) from 550 to 1200 °C; the low-temperature expansion from 0 to 550 °C is shown inset. For both cases, the expansion is relative to the lattice constant at the initial temperature of 0 and 550 °C, respectively. The experimental data of Weiher and Ley,[37] Kundra and Ali,[38] and Solov'eva[17] are drawn for comparison.

temperature range, the quadratic α' term is ca. $5 \times 10^{-10}\,^{\circ}\mathrm{C}^{-2}$ and therefore does not contribute significantly to the thermal expansion (lowering the value of our α to ca. $5.3\,^{\circ}\mathrm{C}^{-1}$, which however is not comparable directly to the linear expansion reported by Solov'eva). The near absence of curvature in the high-temperature regime is therefore consistent with the measurements of Solov'eva, but in contrast to the earlier experiments; the influence of intrinsic defects on the lattice expansion will be explored in further detail below.

A related quantity which we will require later, is the volume thermal-expansion coefficient,

$$\alpha_v = \frac{1}{V}\left(\frac{\partial V}{\partial T}\right)_p, \tag{4}$$

which can be determined from the relation $\alpha_v(T) = 3\alpha_l(T)$, where $\alpha_l(T) = \alpha + 2\alpha' T$.

3. Heat Capacity

To provide further confidence in the description of the thermoelastic properties from our potential model, we have calculated the isobaric heat capacity, $C_p = (\frac{\partial H}{\partial T})_p$. Detailed experimental measurements have been performed, with a reported standard value of $C_p^{\circ} = 99$ J mol^{-1}K^{-1}(see Ref. 62); our model predicts a value of 102 J mol^{-1}K^{-1} in very good agreement.

The thermal-expansion coefficient can be related to the heat capacity:

$$\alpha_v = \gamma \beta_T C_v, \tag{5}$$

where γ is the Grüneisen parameter, which is commonly used to characterise the extent of anharmonicity in the thermoelastic crystal properties, and β_T is the isothermal compressibility of the host lattice $[-\frac{1}{V}(\frac{\partial V}{\partial P})_T]$. The potential model has been shown to reproduce accurately the high-pressure phase transitions of In_2O_3, and the order of stability of several metastable sesquioxide phases;[15] therefore, we expect that the anharmonic contributions to the potential-energy surface are well described. Moreover, the close agreement between the measured and calculated values of the heat capacity and compressibility suggests that the calculated thermal expansion could be closer to the true expansion of the perfect material, whereas the measurements are made for the defect-containing solid.

B. Temperature-dependent (isochoric) defect-reaction energies

The formation energy (U_d) for anion Frenkel-pair formation is 3.19 eV at T = 0 K, which refers to the two defect species at infinite separation (see Eq. (2)). We can also consider the situation where the two components form a bound pair (without recombination),

$$\mathrm{V_O^{\bullet\bullet}} + \mathrm{O_i^{//}} \rightleftharpoons [\mathrm{V_O^{\bullet\bullet}} + \mathrm{O_i^{//}}]^{\times}. \tag{6}$$

The bound Frenkel-pair energy is 2.29 eV for both defects aggregated within the same system at their lowest energy positions; the oxygen vacancy and interstitial are aligned in the ⟨110⟩ direction at a nominal separation of ca. 4 Å. The corresponding defect binding energy can be defined as

$$\Delta E_{\mathrm{Binding}} = E[\mathrm{V_O^{\bullet\bullet}}] + E[\mathrm{O_i^{//}}] - [\mathrm{V_O^{\bullet\bullet}} + \mathrm{O_i^{//}}]^{\times}, \tag{7}$$

which will be positive due to the Coulombic attraction of oppositely charged defects ($\Delta E_{\mathrm{Coulomb}} = -\frac{q^2}{\epsilon_S r}$) and the stabilizing effects of the lattice relaxation in the bound system. A strong binding energy of 1.80 eV is observed for the anion Frenkel pair; $\Delta E_{\mathrm{Coulomb}}$ contributes 1.59 eV to the binding, which is further strengthened due to inefficient screening over small distances.[64,65] For the determination of equilibrium defect concentrations, the energy gain for the formation of the bound complex will be compensated by the loss of configurational entropy.[66]

Taking our predicted thermal expansion for the bulk material, we can study the effect of temperature on defect formation by calculating a given reaction energy as a function of the effective lattice constant at that temperature. Here, we obtain the temperature-dependent internal energy as a sum of internal lattice energy (U_0) and internal vibrational energy (U_{vib}) in the limit of small oscillations:

$$U(T) = U_0(T) + U_{\mathrm{vib}}(T), \tag{8}$$

where,

$$U_{\mathrm{vib}}(T) = \sum_{i=1}^{3N} \frac{\hbar\omega_i}{2} + \left(\frac{\hbar\omega_i}{e^{\hbar\omega_i/k_B T} - 1}\right), \tag{9}$$

or equivalently,

$$U_{\mathrm{vib}}(T) = \sum_{i=1}^{3N} \frac{\hbar\omega_i}{2} \coth\left(\frac{\hbar\omega_i}{2k_B T}\right). \tag{10}$$

In addition to structural effects, the influence of temperature on defect formation will have a contribution from the changes in dielectric properties. From 0 to 1500 K, the static dielectric constant (ϵ_S) increases from 9.05 to 9.62 (+6%), which will mildly dampen the binding energies through a reduced Coulombic attraction; for a doubly charged complex bound at 4 Å, the electrostatic contribution to the binding energy would decrease from 1.59 to 1.50 eV.

The temperature-dependent defect formation energies are listed in Table II and plotted in Fig. 3. At high temperatures, the energy for isolated anion Frenkel-pair formation is reduced from 3.19 (T = 0 K) to 3.02 eV (T = 1500 K), which is largely due to contributions from the oxygen interstitial ($\Delta U_d = -0.29$ eV), whereas the oxygen vacancy exhibits a weaker temperature dependence ($\Delta U_d = -0.04$ eV). Expansion of the lattice is favorable for the formation of both component O_i and $\mathrm{V_O}$ defects. On formation of the bound Frenkel-defect pair, there is a small reduction in the temperature dependence ($\Delta U_d = -0.14$ eV from 0 to 1500 K), which indicates that the bound complex is less sensitive to the local bulk host environment.

C. Temperature-dependent (isochoric) defect reaction entropies and Helmholtz free energies

As with the defect formation energy, the change in vibrational entropy in a defect reaction can be defined as the difference between the vibrational entropies of the bulk and defective systems:

$$S_d = S(\mathrm{defect}) - S(\mathrm{bulk}), \tag{11}$$

TABLE II. Temperature-dependent defect reaction energies (U_d), enthalpies (H_d), and Helmholtz free energies (A_d) for the formation of anion Frenkel pairs in In_2O_3. All values are given in eV per defect.

Temperature (K)	Isolated-Pair Energy (U_d)	Bound-Pair Energy (U_d)	Isolated-Pair Enthalpy (H_d)	Bound-Pair Enthalpy (H_d)	Isolated-Pair Free Energy (A_d)	Bound-Pair Free Energy (A_d)
0	3.19	2.29	3.19	2.29	3.19	2.29
300	3.18	2.28	3.21	2.31	3.14	2.26
600	3.15	2.25	3.21	2.31	3.07	2.21
900	3.11	2.22	3.22	2.32	3.00	2.16
1200	3.07	2.18	3.22	2.32	2.92	2.11
1500	3.02	2.15	3.23	2.33	2.84	2.06
Δ (0–1500)	− 0.17	− 0.14	0.06	0.04	− 0.35	− 0.23

where S is calculated from a sum over all $3N$ vibrational modes (ω_i) of the system (region I of the Mott-Littleton embedded-cluster). In the present case, we calculate S analytically from the derivative of the vibrational component of the Helmholtz free energy (A_{vib}) with respect to temperature:

$$S_v = -\left(\frac{\partial A_{\text{vib}}}{\partial T}\right)_v, \tag{12}$$

where A_{vib} is calculated from:

$$A_{\text{vib}} = k_B T \sum_{i=1}^{3N} \ln\left(2\sinh\frac{\hbar\omega_i}{2k_B T}\right), \tag{13}$$

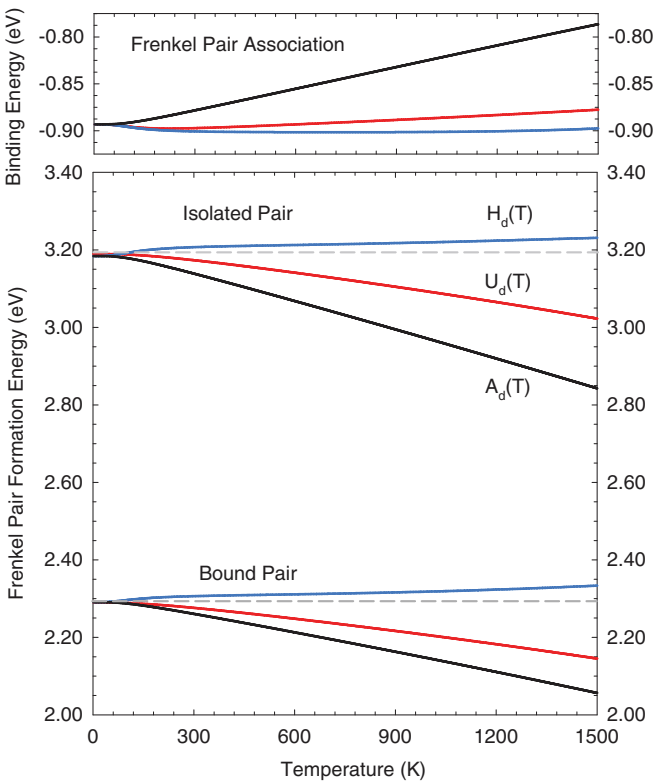

FIG. 3. (Color online) Temperature-dependent defect formation (isochoric) internal (U_d) and free (A_d) energies, and (isobaric) enthalpies (H_d) for isolated and bound anion Frenkel pairs in In_2O_3. All values, including the energies of association, are presented in eV per defect.

resulting in

$$S_v = \sum_{i=1}^{3N} \frac{\hbar\omega_i}{2T}\coth\left(\frac{\hbar\omega_i}{2k_B T}\right) - \frac{A_{\text{vib}}}{T}. \tag{14}$$

In the classical high-temperature (Dulong-Petit) limit, where $T >> \Theta_D$ and Θ_D is the Debye temperature, this reduces to the more familiar form, which has been used elsewhere,[35,40]

$$S_v = k_B \sum_{i=1}^{3N}\left(1 - \ln\frac{\hbar\omega_i}{k_B T}\right). \tag{15}$$

The vibrational entropy contributions to defect formation are listed in Table III. While O_i formation results in additional vibrations (an entropy increase), V_O formation results in a loss of vibrations (an entropy decrease). As an anion Frenkel pair consists of two component defects, the resultant entropy change is small: $2.889k_B$ and $1.493k_B$ for the isolated and bound pairs, respectively, for T = 1000 K. Similar entropic dampening would also be expected for oxidation or reduction reactions, where gaseous oxygen is exchanged with the system. The temperature dependence of the calculated defect entropy is shown in Fig. 4; for each case, the entropies approach their limiting values around 300 K.

From U_d and S_v (both isochoric quantities), the Helmholtz free energy of defect reaction can be calculated directly from $A_d = U_d - TS_v$. The addition of the entropic contributions further enhances the temperature dependence of U_d, with a decrease in the Helmholtz free energy of 0.35 eV for the isolated Frenkel pair and 0.23 eV for the bound pair from 0 to 1500 K, as shown in Fig. 3. The inclusion of vibrational entropy in the free energy of formation also results in a notable decrease in the energy of association for the anion Frenkel pair for higher temperatures: the vibrational entropy is dampened for the bound complex by more than $1k_B$.

TABLE III. Predicted isochoric (S_v) and isobaric (S_p) vibrational entropy contributions associated with Frenkel pair formation in In_2O_3 at T = 1000 K.

Defect	$S_v(k_B)$	$S_p(k_B)$
$V_O^{\bullet\bullet}$	− 3.083	− 2.860
$O_i^{//}$	5.972	8.649
Isolated Frenkel pair	2.889	5.789
Bound Frenkel pair	1.493	4.000

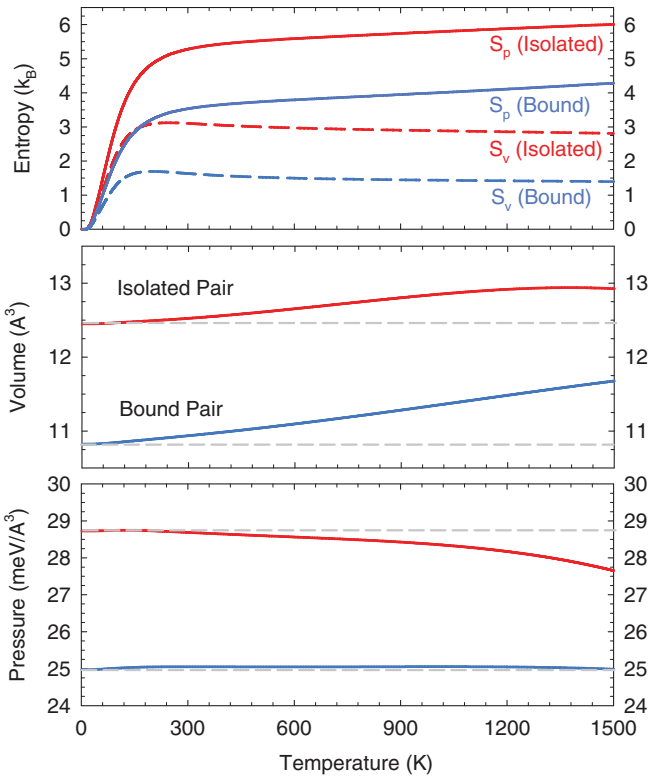

FIG. 4. (Color online) The predicted temperature dependence for three of the thermodynamic parameters associated with Frenkel-pair formation in In_2O_3 from 0 to 1500 K.

The entropic contributions to oxygen vacancy and interstitial formation have recently been calculated for In_2O_3 on the basis of periodic DFT calculations,[67] with predicted values of 2.55 $(-2.82)k_B$ and 2.72 $(11.18)k_B$, respectively, at T = 1000 K under isochoric (isobaric) conditions. Due to the relatively small supercell sizes employed and the resulting electrostatic and elastic finite-size errors, it is difficult to make a quantitative comparison of the two studies; however, our results agree qualitatively with their values obtained under constant-pressure conditions.

The magnitude of the entropic contributions is similar to the values reported in previous studies for solid-state materials.[40] One recent study[68] addressed the effect of lattice vibrations on the diffusion of point defects in silicon carbide, which allows for the calculation of both absolute diffusion rates as well as vibrational entropy contributions to the activation energy for diffusion; the latter contributions were found to be as large as $4k_B$ and to exhibit an appreciable temperature dependence, which is in good agreement with the present findings.

D. Temperature-dependent (isobaric) defect reaction enthalpies and Gibbs free energies

1. Defect pressure

In order to quantify isobaric defect reactions and to extract formation enthalpies, we must explicitly consider the pressure change on defect formation, which is especially important at higher temperatures, where defect concentrations are larger. Following the approach of Catlow *et al.*,[32] which has been described in detail by Gillan and Lidiard[34] and Harding,[35,36] we are conceptually introducing one further point defect into a macroscopic system already containing n noninteracting defects. The primary thermodynamic relationship employed is

$$H_d = U_d - T\left(\frac{\partial V}{\partial T}\right)_p \left(\frac{\partial A_d}{\partial V}\right)_T, \tag{16}$$

where U_d and H_d refer to the temperature-dependent isochoric and isobaric processes, respectively. The second term contains the contribution from the effective defect-formation pressure (p_d), which can be extracted from the derivative of the defect free energy with respect to volume:

$$p_d = -\left(\frac{\partial A_d}{\partial V}\right)_T. \tag{17}$$

In previous studies,[32,34] an equivalent formulation of Eq. (16) has been used to account for the thermal expansion (which was not modeled explicitly):

$$H_d = U_d + p_d \Delta V, \tag{18}$$

where ΔV represents the temperature-dependent lattice volume expansion, which could be calculated from the thermal expansion coefficient (α_v):

$$\Delta V = T\left(\frac{\partial V}{\partial T}\right)_p = \alpha_v T V. \tag{19}$$

In contrast to the formation energy *decrease*, the formation enthalpies *increase* as a function of temperature as shown in Fig. 3. The demonstrated decrease of U_d at higher temperatures is offset by the expansion work involved in the defect reaction. From 0 to 1500 K, an increase of 0.06 eV is predicted for isolated Frenkel pairs. On formation of a bound pair, this effect is slightly dampened to 0.05 eV. The temperature dependence of the defect pressures is found to be small, as shown in Fig. 4.

2. Gibbs free energy

The remaining component required for the calculation of the Gibbs free energy of defect reaction ($G_d = H_d - TS_d$) is the isobaric entropy change. We can use the relation[35,36]

$$S_p = S_v - \left(\frac{\partial V}{\partial T}\right)_p \left(\frac{\partial A_d}{\partial V}\right)_T. \tag{20}$$

The correction term is the same as that used to perform the U_d to H_d conversion [see Eq. (16)]. For Frenkel-pair formation, the isobaric entropy contribution increases from 2.889 to $5.789k_B$ at 1000 K (Table IV), and a similar temperature dependence is found as for the isochoric entropies, except for a slow rise at higher temperatures, which follows the thermal expansion of the In_2O_3 lattice.

A result of the relationships between S_p and S_v [see Eq. (20)] and H_d and U_d [see Eq. (16)], which are valid for a point defect introduced into a macroscopic crystal where the number of lattice sites are conserved, is that $G_d = A_d$ to first order in the defect pressure, p_d. Here, the elastic contributions present in the entropic and enthalpic terms of G_d cancel. When describing a change in the number of lattice sites (e.g., Schottky disorder), an additional term is required;[69] however, it is not needed for the case of Frenkel disorder.

TABLE IV. Predicted pressure change, and corresponding defect volume and effective radius, associated with Frenkel-pair formation in In_2O_3 at T = 1000 K.

Defect	Pressure (GPa)	Pressure (eV/Å^3)	Volume (Å^3)	Radius (Å)
$V_O^{\bullet\bullet}$	0.35	0.0022	0.99	0.62
$O_i^{//}$	4.20	0.0262	11.86	1.41
Isolated Frenkel pair	4.55	0.0284	12.85	1.45
Bound Frenkel pair	4.02	0.0251	11.35	1.39

For finite defect concentrations, such as those present for calculations performed within the supercell approach, the relationship $G_d = A_d$ does not hold true, owing to the fact that the defect center is embedded not in a macroscopic crystal but in a defective one. The first-order correction, which is dependent on the supercell expansion (or defect concentration, $n = 1/v_{\text{supercell}}$) is[70]

$$G_d = A_d - \frac{1}{2}\left(\frac{v_d}{v_{\text{supercell}}}\right) p_d V, \tag{21}$$

where v_d is the defect volume of formation, to be described below.

3. *Defect-induced lattice expansion*

From the calculated data, we can also assess the effective volume associated with point-defect formation. Removal of the increment of pressure caused by isochoric defect formation (p_d) has an associated isobaric volume change (v_d). Through a relation analogous to Hooke's law of elasticity:

$$v_d = -p_d\left(\frac{\partial V}{\partial P}\right)_T = p_d \beta_T V, \tag{22}$$

where V is the temperature-dependent bulk cell volume. The pressures and volumes of defect formation for each species are listed in Table IV. At T = 1000 K, the volumes of formation for the isolated and bound Frenkel pairs are 12.85 and 11.35 Å^3, respectively. Assuming an isotropic (spherical) dilation, the corresponding defect radii are 1.45 and 1.39 Å. Similar to the defect pressures, the defect volumes do not exhibit a significant temperature dependence; the values increase as a function of temperature due to a softening of the crystal lattice (increase in compressibility).

Neglecting long-range defect interactions, the volume of the defective cell can therefore be calculated for an arbitrary concentration (per unit cell) of defect species as

$$V_d = V + n v_d. \tag{23}$$

The resulting plot of the lattice strain against Frenkel pair concentration is shown for $T = 1500$ K in Fig. 5, which demonstrates that Frenkel pairs can contribute to the lattice expansion if produced in sufficient concentrations, which may be the case in In_2O_3 as disorder in the anion sublattice is known to occur at higher temperatures. Indeed, to account for the differences in the calculated thermal expansion and the experimental values (see Fig. 2), Frenkel-pair concentrations of 2×10^{19} cm^{-3} (Solov'eva[37]), 1×10^{21} cm^{-3} (Kundra and Ali[38]), and 2×10^{21} cm^{-3} (Weiher and Ley[37]) would be required.

It has been predicted that oxygen vacancies have a low formation energy,[9,10,12] which could lead to nonstoichiometry (i.e., $In_2O_{3-\delta}$); however, because the defect volume of $V_O^{\bullet\bullet}$ is remarkably small ($v_d = 0.99$ Å^3 and the effective defect radius is 0.62 Å), isolated vacancies will *not* contribute significantly to the lattice expansion. To explain the high-temperature lattice expansion and the large variation in the oxygen partial-pressure dependence of the electrical conductivity, in addition to isolated oxygen vacancies, more complex defect compensation or aggregation must occur in In_2O_3, where oxygen interstitials are undoubtedly involved.

IV. DISCUSSION

As we have demonstrated above, all of the principal thermodynamic parameters associated with point-defect formation can be obtained using a well-defined computational procedure:

(1) Isochoric defect formation performed at the equilibrium (T = 0 K) lattice constant yields the reaction energies and entropies $U_d(0)$ and $S_v(0)$.

(2) Isochoric defect formation performed as a function of the lattice constant yields temperature-dependent $U_d(T)$ and $S_v(T)$, and therefore, the temperature-dependent Helmholtz free energy of formation ($A_d = U_d - TS_v$), which is equivalent to the Gibbs free energy at the limit of infinite dilution.

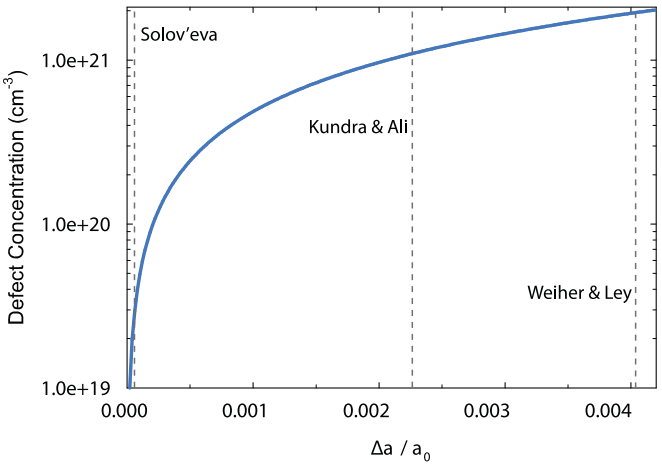

FIG. 5. (Color online) The predicted lattice strain of In_2O_3 as a function of Frenkel-pair concentration, for T = 1500 K and assuming negligible interactions between defect species. The dashed vertical lines refer to the differences in thermal expansion between the calculated value and the experimental reports of Weiher and Ley,[37] Kundra and Ali,[38] and Solov'eva.[17]

(3) The pressure of defect formation, $p_d = -(\frac{\partial A_d}{\partial V})_T$, can be obtained through differentiation of the temperature-dependent Helmholtz free energy.

(4) Modeling of the bulk thermoelastic properties yields the bulk isothermal compressibility [$\beta_T = -\frac{1}{V}(\frac{\partial V}{\partial P})_T$], which allows for the calculation of temperature-dependent defect reaction enthalpies through the relation: $H_d = U_d - T(\frac{\partial V}{\partial T})_p(\frac{\partial A_d}{\partial V})_T$.

(5) The volume of defect formation, $v_d = -p_d(\frac{\partial V}{\partial P})_T$, can then be obtained through the previously determined values of p_d and β_T.

(6) Finally, relating the isochoric and isobaric defect entropies [$S_p = S_v - (\frac{\partial V}{\partial T})_p(\frac{\partial A_d}{\partial V})_T$] gives access to the Gibbs free energy of defect formation, $G_d = H_d - TS_p$, which is appropriate for modeling finite defect concentrations.

Our calculations have clearly shown that the temperature dependence of the thermodynamic parameters governing defect formation is appreciable. Furthermore, consideration of temperature-dependent defect formation energies can have significant influence on the thermodynamic stability and will be of particular relevance for modeling equilibrium defect and carrier concentrations under different experimental growth conditions. While the present study has been restricted to the embedded-cluster Mott-Littleton method, in principle the same approach can be applied to periodic supercell calculation of defects, e.g., as in Refs. 70 and 71; however, careful attention must be paid to achieve appropriate convergence in the cell sizes, especially for charged defect centers.

Concerning the high-temperature thermal expansion of indium oxide, our calculations demonstrate that while oxygen vacancies alone will not contribute appreciably to lattice expansion, charge compensation by oxygen interstitials, producing anion Frenkel pairs, will effect a significant free volume of defect formation and hence can contribute to the lattice expansion when produced in significant abundance. Making the strong assumption that the Frenkel pair is the only defect present in the system, the variation in thermal expansion observed at high temperatures (Fig. 2) could be accounted for by Frenkel-pair formation involving concentrations of the order of 10^{19} cm^{-3}. Such a high degree of disorder in the anion sublattice is not unrealistic considering the structural freedom offered by the bixbyite structure and the typical carrier concentrations of the undoped material, which can exceed 10^{21} cm^{-3}[1]. However, such concentrations are above the thermodynamic limit set by the formation energy of the isolated Frenkel pairs, i.e., $n = N_{\text{sites}}\exp(-\frac{G_d}{k_B T})$, which again suggests that more complex defect aggregates are at play, probably involving oxygen exchange and/or redox reactions at the material surface and grain boundaries. Further experimental and theoretical investigations could help to verify these predictions.

V. CONCLUSIONS

We have investigated the thermodynamics of anion Frenkel-pair formation in In_2O_3 with an analytical interatomic potential, within the Mott-Littleton embedded-cluster approach. Temperature and pressure effects are found to make significant contributions to the thermodynamics of defect formation and, within the approximations of the given model, can change the reaction energies by up to 0.4 eV. Furthermore, anion Frenkel pairs are likely to contribute to the high-temperature thermal expansion of In_2O_3, while isolated oxygen vacancies are not, due to a low free volume of defect formation. We note that the low-temperature thermal expansion of indium oxide has not been studied experimentally, and the discrepancy between experimental and theoretical data in the intermediate regime (0–550 °C) warrants further investigation. We have demonstrated that the calculation of the full free-energy expansion of defect formation including enthalpic and entropic effects is possible using a well-defined computational procedure, which should facilitate future studies of defect formation and behavior in solid-state systems.

ACKNOWLEDGMENTS

We would like to thank Scott M. Woodley and Stephen A. Shevlin for useful discussions. A.W. acknowledges funding from the Marie-Curie scheme of the European Union under the Seventh Framework Programme. The authors acknowledge the use of the UCL Legion High Performance Computing (HPC) Facility, and associated support services, in the completion of this work. The work has also been supported by an EPSRC Portfolio Partnership (Grant No. ED/D504872) and membership of the UK's HPC Materials Chemistry Consortium, which is funded by EPSRC (Grant No. EP/F067496).

*a.walsh@bath.ac.uk

[1] P. P. Edwards, A. Porch, M. O. Jones, D. V. Morgan, and R. M. Perks, Dalton Trans. **15**, 2995 (2004).
[2] I. Hamberg, C. G. Granqvist, K. F. Berggren, B. E. Sernelius, and L. Engstrom, Phys. Rev. B **30**, 3240 (1984).
[3] I. Hamberg and C. G. Granqvist, J. Appl. Phys. **60**, R123 (1986).
[4] A. Walsh, J. L. F. Da Silva, S.-H. Wei, C. Körber, A. Klein, L. F. J. Piper, A. DeMasi, K. E. Smith, G. Panaccione, P. Torelli, D. J. Payne, A. Bourlange, and R. G. Egdell, Phys. Rev. Lett. **100**, 167402 (2008).
[5] J. H. W. DeWit, J. Solid State Chem. **20**, 143 (1977).
[6] Y. Ohya, T. Yamamoto, and T. Ban, J. Am. Ceram. Soc. **91**, 240 (2008).
[7] J. H. W. DeWit, J. Solid State Chem. **8**, 142 (1973).
[8] R. L. Weiher, J. Appl. Phys. **33**, 2834 (1962).
[9] S. Lany and A. Zunger, Phys. Rev. Lett. **98**, 045501 (2007).
[10] P. Ágoston, P. Erhart, A. Klein, and K. Albe, J. Phys. Condens. Matter **21**, 455801 (2009).
[11] T. Tomita, K. Yamashita, Y. Hayafuji, and H. Adachi, Appl. Phys. Lett. **87**, 051911 (2005).
[12] P. Ágoston, K. Albe, R. M. Nieminen, and M. J. Puska, Phys. Rev. Lett. **103**, 245501 (2009).

[13] J. E. Medvedeva and C. L. Hettiarachchi, Phys. Rev. B **81**, 125116 (2010).
[14] P. Ágoston and K. Albe, Phys. Rev. B **81**, 195205 (2010).
[15] A. Walsh, C. R. A. Catlow, A. A. Sokol, and S. M. Woodley, Chem. Mater. **21**, 4962 (2009).
[16] A. Walsh and S. M. Woodley, Phys. Chem. Chem. Phys. **12**, 8446 (2010).
[17] A. E. Solov'eva, Ogneupory **7**, 22 (1987).
[18] G. Frank and H. Kostlin, Appl. Phys. A **27**, 197 (1982).
[19] S. B. Zhang, S.-H. Wei, A. Zunger, and H. Katayama-Yoshida, Phys. Rev. B **57**, 9642 (1998).
[20] D. O. Scanlon, B. J. Morgan, G. W. Watson, and A. Walsh, Phys. Rev. Lett. **103**, 096405 (2009).
[21] A. A. Sokol, S. A. French, S. T. Bromley, C. R. A. Catlow, H. J. J. van Dam, and P. Sherwood, Faraday Discuss. **134**, 267 (2007).
[22] A. Walsh, J. L. F. Da Silva, and S.-H. Wei, Phys. Rev. B **78**, 075211 (2008).
[23] A. Alkauskas, P. Broqvist, and A. Pasquarello, Phys. Rev. Lett. **101**, 046405 (2008).
[24] C. W. M. Castleton, A. Höglund, and S. Mirbt, Phys. Rev. B **73**, 035215 (2006).
[25] P. Erhart, K. Albe, and A. Klein, Phys. Rev. B **73**, 205203 (2006).
[26] A. Janotti and C. G. Van de Walle, Phys. Rev. B **76**, 165202 (2007).
[27] A. Walsh, S.-H. Wei, Y. Yan, M. M. Al Jassim, J. A. Turner, M. Woodhouse, and B. A. Parkinson, J. Phys. Chem. C **112**, 12044 (2008).
[28] A. Walsh, J. Phys. Chem. Lett. **1**, 1284 (2010).
[29] C. R. A. Catlow, Z. X. Guo, M. Miskufova, S. A. Shevlin, A. G. H. Smith, A. A. Sokol, A. Walsh, D. J. Wilson, and S. M. Woodley, Philos. Trans. R. Soc. London A **368**, 3379 (2010).
[30] N. F. Mott and R. W. Gurney, *Electronic Processes in Ionic Crystals*, 2nd ed. (Oxford University Press, Oxford, 1948).
[31] C. R. A. Catlow, J. Corish, and P. W. M. Jacobs, J. Phys. C **12**, 3433 (1979).
[32] C. R. A. Catlow, J. Corish, P. W. M. Jacobs, and A. B. Lidiard, J. Phys. C **14**, 121 (1981).
[33] C. R. A. Catlow, J. Corish, K. M. Diller, P. W. M. Jacobs, and M. J. Norgett, J. Phys. C **12**, 451 (1979).
[34] M. J. Gillan and A. B. Lidiard, *in Characteristic Volumes of Point Defects in Ionic Crystals, Lecture Notes in Physics*, Vol. 166 (Springer, Berlin, 1982).
[35] J. H. Harding, Phys. Rev. B **32**, 6861 (1985).
[36] J. H. Harding, J. Chem. Soc., Faraday Trans. **2**, 351 (1989).
[37] R. L. Weiher and R. P. Ley, J. Appl. Phys. **34**, 1833 (1963).
[38] K. D. Kundra and S. Z. Ali, J. Appl. Crystallogr. **3**, 543 (1970).
[39] H. B. Huntington, G. A. Shirn, and E. S. Wajda, Phys. Rev. **99**, 1085 (1955).
[40] P. W. M. Jacobs, M. A. Nerenberg, and J. Govindarajan, *in Theory and Calculation of Defect Entropies, Lecture Notes in Physics*, Vol. 166 (Springer, Berlin, 1982).
[41] M. J. Gillan, J. H. Harding, and M. Leslie, J. Phys. C **21**, 5465 (1988).
[42] B. Grabowski, L. Ismer, T. Hickel, and J. Neugebauer, Phys. Rev. B **79**, 134106 (2009).
[43] J. D. Gale and A. L. Rohl, Mol. Simul. **29**, 291 (2003).
[44] L. N. Kantorovich, Phys. Rev. B **51**, 3520 (1995).
[45] L. N. Kantorovich, Phys. Rev. B **51**, 3535 (1995).
[46] H. J. Monkhorst and J. D. Pack, Phys. Rev. B **13**, 5188 (1976).
[47] N. F. Mott and M. J. Littleton, Trans. Faraday Soc. **34**, 485 (1938).
[48] A. A. Sokol, S. T. Bromley, S. A. French, C. R. A. Catlow, and P. Sherwood, Int. J. Quantum Chem. **99**, 695 (2004).
[49] P. Sherwood, A. H. deVries, M. F. Guest, G. Schreckenbach, C. R. A. Catlow, S. A. French, A. A. Sokol, S. T. Bromley, W. Thiel, A. J. Turner, S. Billeter, F. Terstegen, S. Thiel, J. Kendrick, S. C. Rogers, J. Casci, M. Watson, F. King, E. Karlsen, M. Sjovoll, A. Fahmi, A. Schafer, and C. Lennartz, J. Mol. Struct. (Theochem.) **632**, 1 (2003).
[50] C. R. A. Catlow, A. A. Sokol, and A. Walsh, Chem. Commun. **47**, 3386 (2011).
[51] W. Kohn and L. J. Sham, Phys. Rev. **140**, A1133 (1965).
[52] P. Hohenberg and W. Kohn, Phys. Rev. **136**, B864 (1964).
[53] G. Kresse and J. Furthmüller, Phys. Rev. B **54**, 11169 (1996).
[54] G. Kresse and J. Furthmüller, Comput. Mater. Sci. **6**, 15 (1996).
[55] G. Kresse and D. Joubert, Phys. Rev. B **59**, 1758 (1999).
[56] J. P. Perdew, A. Ruzsinszky, G. I. Csonka, O. A. Vydrov, G. E. Scuseria, L. A. Constantin, X. Zhou, and K. Burke, Phys. Rev. Lett. **100**, 136406 (2008).
[57] F. D. Murnaghan, Proc. Natl. Acad. Sci. USA **30**, 244 (1944).
[58] S. Baroni, S. de Gironcoli, A. Dal Corso, and P. Giannozzi, Rev. Mod. Phys. **73**, 515 (2001).
[59] F. Fuchs and F. Bechstedt, Phys. Rev. B **77**, 155107 (2008).
[60] M. Marezio, Acta Crystallogr. **20**, 723 (1966).
[61] D. Liu, W. W. Lei, B. Zou, S. D. Yu, J. Hao, K. Wang, B. B. Liu, Q. L. Cui, and G. T. Zou, J. Appl. Phys. **104**, 083506 (2008).
[62] E. H. P. Cordfunke and E. F. Westrum, J. Phys. Chem. Solids **53**, 361 (1992).
[63] K.-P. Bohnen, R. Heid, L. Pintschovius, A. Soon, and C. Stampfl, Phys. Rev. B **80**, 134304 (2009).
[64] F. A. Kröger, *The Chemistry of Imperfect Crystals*, Vol. 2, 2nd ed. (North-Holland, Amsterdam, 1974).
[65] If instead the high frequency dielectric constant is used, the anticipated Coulomb binding would be 3.7 eV; therefore, the present case lies in between. Association effects are discussed in detail in Chapter 10 of Ref. 64.
[66] D. M. Smyth, *The Defect Chemistry of Metal Oxides* (Oxford University Press, Oxford, 2000).
[67] P. Ágoston and K. Albe, Phys. Chem. Chem. Phys. **11**, 3226 (2009).
[68] O. N. Bedoya-Martínez and G. Roma, Phys. Rev. B **82**, 134115 (2010).
[69] M. J. Gillan, Philos. Mag. **43**, 301 (1981).
[70] M. B. Taylor, G. D. Barrera, N. L. Allan, T. H. K. Barron, and W. C. Mackrodt, Faraday Discuss. **106**, 377 (1997).
[71] S. C. Parker and G. D. Price, in *Advances in Solid-State Chemistry*, Vol. 1 (JAI Press, Stamford, 1989).